

Magnetocapacitance oscillations and thermoelectric effect in two-dimensional electron gas irradiated by microwaves.

A. D. Levin,¹ G. M. Gusev,¹ O. E. Raichev,² Z. S. Momtaz,¹ and A. K. Bakarov,^{3,4}

¹*Instituto de Física da Universidade de São Paulo, 135960-170, São Paulo, SP, Brazil*

²*Institute of Semiconductor Physics, NAS of Ukraine, Prospekt Nauki 41, 03028 Kyiv, Ukraine*

³*Institute of Semiconductor Physics, Novosibirsk 630090, Russia and*

⁴*Novosibirsk State University, Novosibirsk 630090, Russia*

(Dated: September 11, 2018)

To study the influence of microwave irradiation on two-dimensional electrons, we apply a method based on capacitance measurements in GaAs quantum well samples where the gate covers a central part of the layer. We find that the capacitance oscillations at high magnetic fields, caused by the oscillations of thermodynamic density of states, are not essentially modified by microwaves. However, in the region of fields below 1 Tesla, we observe another set of oscillation, with the period and the phase identical to those of microwave induced resistance oscillations. The phenomenon of microwave induced capacitance oscillations is explained in terms of violation of the Einstein relation between conductivity and the diffusion coefficient in the presence of microwaves, which leads to a dependence of the capacitor charging on the anomalous conductivity. We also observe microwave-induced oscillations in the capacitive response to periodic variations of external heating. These oscillations appear due to the thermoelectric effect and are in antiphase with microwave induced resistance oscillations because of the Corbino-like geometry of our experimental setup.

PACS numbers: 73.43.Qt, 73.50.Pz, 73.21.Fg, 73.50.Lw

I. INTRODUCTION

The microwave (MW) irradiation of high-mobility two-dimensional (2D) electron gas in the perpendicular magnetic field B dramatically modifies the transport properties of the electron system and leads to a remarkable phenomenon of microwave-induced resistance oscillations (MIRO) and associated zero resistance states [1-3]. The periodicity of the oscillations is determined by the ratio of the MW frequency ω to the cyclotron frequency $\omega_c = |e|B/mc$ (m is the effective mass of the electron). Whereas the physics of MIRO is not fully understood, the majority of experimentally observed features are described [3-9] by the theories based on the consideration of scattering-assisted transitions of electrons between Landau levels due to absorption and emission of MW radiation quanta. Besides, purely classical approaches to magnetotransport [10 - 13] were also applied to the description of the phenomenon, and it was suggested that MIRO might originate from the effects near sample edges [11,12] and contacts [12] as opposed to the bulk transport properties.

The progress in understanding the effect of MW irradiation on 2D electrons in general and the MIRO phenomenon in particular crucially depends on the information obtained from experimental studies, which in turn relies on the diversity of applied experimental methods. The basic method is a standard magnetotransport experiment, the measurements of electrical resistance under external dc driving. The methods that do not use dc driving are rare exceptions. They include measurements of the photovoltaic response in the samples with built-in spatial variation of electron density near the contacts [14 - 16], when the oscillating photovoltage appears as

a result of MW irradiation, and thermoelectric measurements [17], when the MW irradiation leads to oscillations of therminduced (phonon-drag) voltage. In this paper, we propose and exploit another method, based on capacitance measurements in the samples where the gate covers a central part of the 2D layer.

Studies of the capacitive response commonly serve as a source of information about the thermodynamic properties of 2D electron gas in magnetic field. In particular, measurements of low-frequency electrical impedance in these systems allow one to find the thermodynamic density of states $(\partial n/\partial \mu)_T$, where n is the electron density and μ is the chemical potential [18 - 23]. This is an efficient method to study the density of states of electrons as well as the correlation effects, which is important for understanding the integer and fractional quantum Hall effects. Recently, it was proposed [24] to apply periodic variations of temperature T , induced by a heater to extract the entropy density $(\partial S/\partial n)_T = -(\partial \mu/\partial T)_n$, which gives complementary information about the properties of 2D electron systems.

Below we show experimentally that both voltaic and thermal perturbations in the presence of MW irradiation lead to an oscillating capacitive response that bears a resemblance to MIRO. A theoretical consideration gives an explanation of these effects, suggesting that the response in both cases is directly related to MW-induced changes in electrical conductivity. In spite of the fact that MW irradiation does not change the carrier density, it causes redistribution of potentials in the 2D plane partly covered by the gate. We establish two physical mechanisms of such influence. First, since the MW irradiation strongly modifies the conductivity and does not change the diffusion coefficient, the Einstein relation be-

comes violated [16]. This leads to a difference between electrochemical potentials in the regions under the gate and out of the gate. Second, in the presence of temperature gradients, the capacitor charging is influenced by the thermoinduced voltage between the Ohmic contact to 2D gas and the heated region under the gate. Meanwhile, it is established that thermoinduced voltages are modified by the MW irradiation [17,25], mostly because of the influence of the radiation on conductivity. It is worth to note that the MW-induced effects described above exist and are actually the most prominent in the region of a relatively weak magnetic field, where the Shubnikov-de Haas oscillations are thermally suppressed. In this region, the magnetic-field induced changes in thermodynamic density of states and in entropy density are not seen experimentally. Therefore, the oscillations of the capacitive response due to MW irradiation are easily separable from the oscillations of thermodynamic quantities which appear at higher magnetic fields.

The paper is organized as follows. In Section II we present the details of measurements and experimental results. Section III contains the theoretical description, comparison of theory with experiment, and discussion. Concluding remarks are given in the last section.

II. EXPERIMENT

We studied Schottky-gated narrow (14 nm) quantum wells (QW) with electron density $n \simeq 6.5 \times 10^{11} \text{ cm}^{-2}$ and a mobility $\mu = 2 \times 10^6 \text{ cm}^2/\text{V s}$. We used square ($8 \times 8 \text{ mm}^2$) specimens of Van der Pauw geometry, with contacts at the corners. A 4.5 nm TiAu semitransparent gate of nearly circular shape with area $A = 4 \text{ mm}^2$ was evaporated on top of the sample. The distance between the QW and the sample surface was $d_G = 115 \text{ nm}$, and the gate-QW geometric capacitance C_0 was 3.9 nF. The capacitance was measured by the modulation technique: the gate voltage was modulated with a small ac voltage of 10-50 mV at frequencies in the range 1.5–3.1 Hz and the recharging current was measured using a lock-in amplifier. The geometric capacitance and the frequencies were small enough to neglect contribution of the resistance of the 2D electron gas in the recharging current signal. We also measured low-frequency ac voltage proportional to the recharging current generated due to temperature modulation by applying a technique similar to that used in Ref. 24. The heater was placed on the back side of the sample in order to minimize the temperature gradient over the sample area. The heater voltage was modulated by the law $v_0 + v_0 \cos(\omega_0 t)$, with $f_0 = \omega_0/2\pi \approx 3.24 \text{ Hz}$, leading to modulation of heating power with the same frequency. The corresponding variation of electron temperature $\Delta T \sim 0.2 \text{ K}$ was estimated from the amplitude of the Shubnikov-de Haas oscillations. The measurements were carried out in a VTI cryostat with a waveguide to deliver microwave (MW) irradiation (frequency range 110 to 170 GHz) down to the sample. Several devices from

the same wafer were studied.

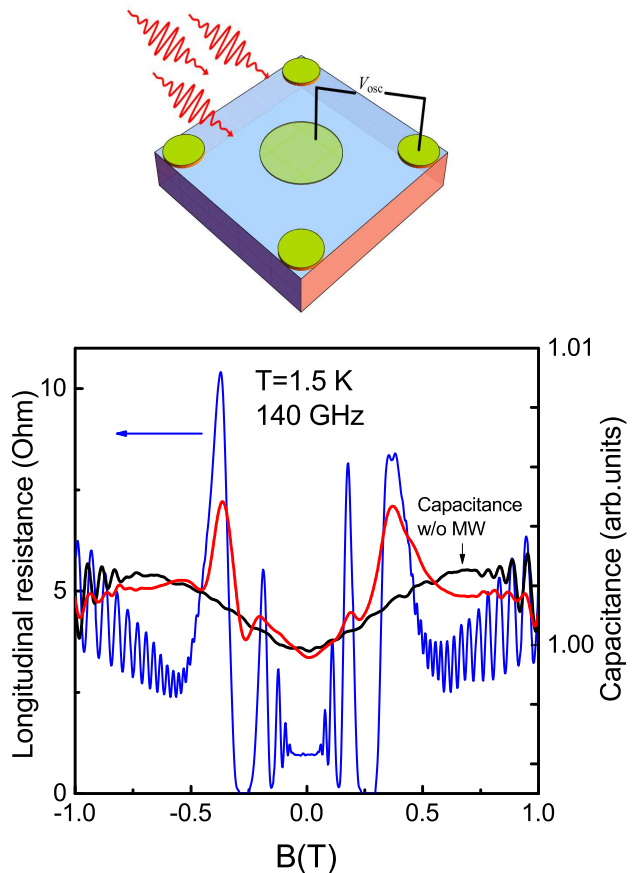


FIG. 1: Magnetoresistance and magnetocapacitance under microwave irradiation of frequency 140 GHz. Dark magnetocapacitance is also shown. The top part shows the geometry of the experiment.

In Fig. 1 we present the longitudinal magnetoresistance under microwave irradiation for 140 GHz and at a temperature of 1.5 K. The resistance reveals strong MIRO and zero resistance state evolved from the last minimum. This figure also shows typical magnetocapacitance (capacitance $C(B)$ normalized to its zero-field value) traces both with MW and without it. The presence of MW irradiation results in an oscillating magnetocapacitance contribution with much weaker relative amplitude in comparison with phototransistance. The period and the phase of the photocapacitance oscillations coincide with those of MIRO, though we do not see any indications of a zero resistance state regime in the main minimum of the capacitance. In Fig. 2 we plot the magnetocapacitance for an extended interval of B in order to show the pronounced oscillations caused by consecutive passage of Landau levels through the Fermi level when the Landau levels become separated in strong magnetic

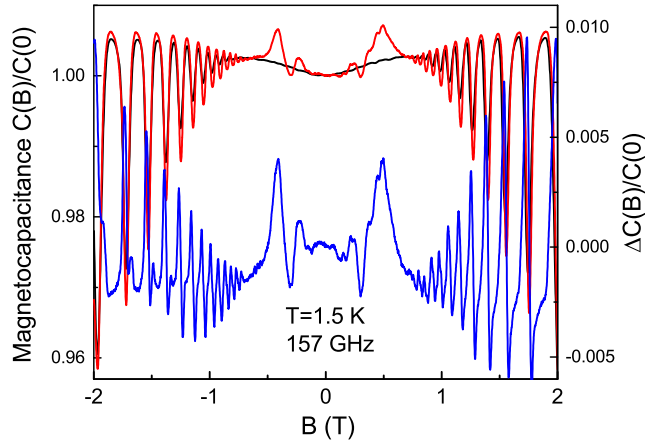


FIG. 2: Magnetocapacitance, dark and under MW irradiation at 157 GHz, in a wide interval of magnetic fields. The lower plot shows the difference ΔC between the MW-induced and dark magnetocapacitances.

fields. The MW irradiation does not lead to a qualitative change of the shape of these oscillations, though the amplitudes slightly increase. We point out that this behavior is not usual, as one should expect some decrease in the amplitudes because of heating of the electron gas by microwaves.

Figure 3 illustrates magnetooscillations of recharging voltage induced by temperature modulation under MW irradiation in comparison with MIRO. The periodicity of these oscillations is the same as that of MIRO. However, in contrast to MW-induced magnetocapacitance oscillations, the oscillations of thermoinduced voltage have a much larger amplitude and occur in antiphase with MIRO. These properties have been checked in the measurements for several different MW frequencies. The charging voltage without MW irradiation (dark signal) demonstrates weak features identified as the magnetophonon oscillations due to resonance scattering of electrons by acoustic phonons. These oscillations were observed previously in phonon-drag thermopower measurements [17,26] as well as in the magnetoresistance of 2D electron systems (see Ref. 3 for a review). The presence of magnetophonon oscillations suggests that the charging is influenced by thermoelectric effects mediated by phonon drag. The oscillating contribution added by MW irradiation is much larger than the magnetophonon oscillations.

III. THEORY AND DISCUSSION

The experimental data presented above show that microwaves have a non-trivial effect on gate-QW capacitor charging. This effect resembles the influence of mi-

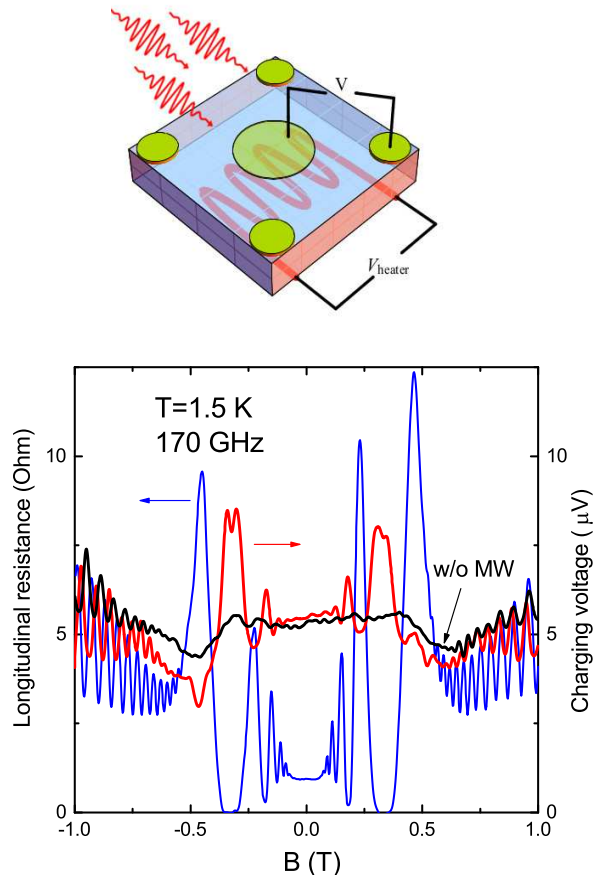


FIG. 3: Magnetoresistance and charging voltage under microwave irradiation of frequency 170 GHz. Dark charging voltage is also shown. The top part shows the geometry of the experiment.

crowaves on resistance and depends on the type of excitation source, whether electric or thermal. The theory given in this section provides a detailed account of the processes contributing to the observed capacitive response.

The recharging current is given by the time derivative of the induced electric charge δQ :

$$J_t = \frac{d\delta Q_t}{dt} = e \int_G d\mathbf{r} \frac{dn_{rt}}{dt}, \quad (1)$$

where n_{rt} is the local electron density and the integral is taken over the region covered by the gate. Below, the time index is dropped out because the recharging occurs in the quasi-stationary regime. The variation of the electrostatic potential in the 2D layer under the gate is related to the variation of the electron density as $\delta\phi = (4\pi e d_G / \epsilon_0) \delta n$, where ϵ_0 is the dielectric permittivity of the cap layer and d_G is the distance between the gate and the 2D layer. Since the electrochemical poten-

tial η , which determines the local voltage $V_{\mathbf{r}} = \eta_{\mathbf{r}}/e$, is connected with electrostatic potential and chemical potential by the relation

$$\eta_{\mathbf{r}} = e\phi_{\mathbf{r}} + \mu_{\mathbf{r}}, \quad (2)$$

the variation of the voltage under the gate is written as

$$e\delta V = \delta\mu + (4\pi e^2 d_G/\epsilon_0)\delta n. \quad (3)$$

In this expression, the coordinate index is dropped out because we consider the quantities averaged over the areas of the size exceeding all microscopic lengths including the screening length, so δn is assumed to be coordinate-independent. The local equilibrium condition (the absence of currents) requires δV to be coordinate-independent if the temperature under the gate is uniform, which is also assumed. Equation (3), with the use of the relation

$$\delta\mu = \frac{\partial\mu}{\partial n}\delta n + \frac{\partial\mu}{\partial T}\delta T$$

leads to electric charge variation as a response to both the voltage and the temperature variations:

$$\delta Q = C[\delta V - e^{-1}(\partial\mu/\partial T)\delta T], \quad (4)$$

with the capacitance

$$C = C_0 \left[1 + \frac{C_0}{e^2 A} \left(\frac{\partial n}{\partial \mu} \right)^{-1} \right]^{-1}, \quad (5)$$

where A is the area under the gate and $C_0 \simeq \epsilon_0 A/4\pi d_G$ is the geometric capacitance.

Therefore, the capacitive response to perturbations δV and δT is described by the isothermic derivative $\partial n/\partial \mu$ and the derivative $\partial\mu/\partial T$ at constant electron density. For non-interacting electron gas in thermodynamic equilibrium, these quantities are entirely described by the density of states in the magnetic field:

$$\frac{\partial n}{\partial \mu} = \rho_{2D} \int d\varepsilon \left(-\frac{\partial f_\varepsilon}{\partial \varepsilon} \right) D_\varepsilon \quad (6)$$

and

$$\frac{\partial \mu}{\partial T} = -\rho_{2D} \left(\frac{\partial n}{\partial \mu} \right)^{-1} \int d\varepsilon \left(-\frac{\partial f_\varepsilon}{\partial \varepsilon} \right) D_\varepsilon \frac{\varepsilon - \mu}{T}, \quad (7)$$

where D_ε is the density of states expressed in units $\rho_{2D} = m/\pi\hbar^2$ and f_ε is the equilibrium distribution function. If the density of states is represented as a series of oscillating harmonics, $D_\varepsilon = 1 + 2 \sum_{k=1}^{\infty} a_k \cos(2\pi k\varepsilon/\hbar\omega_c)$, these expressions are rewritten as

$$\frac{\partial n}{\partial \mu} = \rho_{2D} S_0, \quad \frac{\partial \mu}{\partial T} = -\frac{S_1}{S_0}, \quad (8)$$

$$S_0 = 1 + 2 \sum_{k=1}^{\infty} a_k \frac{X_k}{\sinh X_k} \cos \left(\frac{2\pi k\mu}{\hbar\omega_c} \right),$$

$$S_1 = 2\pi \sum_{k=1}^{\infty} a_k \frac{\partial}{\partial X_k} \frac{X_k}{\sinh X_k} \sin \left(\frac{2\pi k\mu}{\hbar\omega_c} \right), \quad (9)$$

where $X_k = 2\pi^2 kT/\hbar\omega_c$. Equation (9) demonstrates the presence of quantum oscillations similar to Shubnikov-de Haas oscillations. Such kind of oscillations are known to be suppressed because of random spatial fluctuations of the chemical potential [27]. If such variations are described by a Gaussian distribution $\propto \exp[-(\mu - \bar{\mu})^2/\Gamma^2]$, their influence can be taken into account by multiplying the terms under the sums in Eq. (9) by the factors $\exp[-(\pi\Gamma k/\hbar\omega_c)^2]$.

Let us discuss in which way the microwaves can modify the quantities $\partial n/\partial \mu$ and $\partial\mu/\partial T$. First of all, the MW irradiation leads to some heating of electron gas and, therefore, suppresses the oscillations as factors X_k increase. This is, however, a trivial effect which we are not interested in below. A very intensive radiation may modify the electron spectrum, but we did not work with such powerful MW sources in our experiment. Also, the MW irradiation creates an additional oscillating part of the distribution function, $\delta f_\varepsilon^{(\omega)}$, which is responsible for the "inelastic" mechanism [7] of MIRO. However, since the radiation does not change the number of electrons in the system, one has the identity $\int d\varepsilon D_\varepsilon \delta f_\varepsilon^{(\omega)} = 0$ which means that both $\partial n/\partial \mu$ and $\partial n/\partial T$ remain unchanged. The quantity $\partial\mu/\partial T$ may change, but the relative contribution of this effect is estimated, from a direct calculation, as $\hbar\omega/\mu$ times smaller than the relative effect of microwaves on the conductivity. Therefore, we conclude that the influence of MW irradiation on the capacitive response through the quantities $\partial n/\partial \mu$ and $\partial\mu/\partial T$ is basically reduced to the effect of heating of the electron gas. Another kind of influence, through the transport properties of the 2D layer, is more essential and considered below.

The response of the system to external perturbations is determined not only by the intrinsic properties of the capacitor between the 2D gas and the gate, but also by the potential distribution in the 2D plane. In other words, knowing the relation Eq. (4) between δQ , δV , and δT is not sufficient to solve the problem since V is the voltage under the gate, while in our sample the contact to the 2D gas is placed outside the gate and stays at a different voltage V_0 . To find a relation between V and V_0 , we present the local current density as

$$\mathbf{j}_{\mathbf{r}} = \mathbf{j}_{\mathbf{r}}^{(0)} + \mathbf{j}_{\mathbf{r}}^{(t)} + \mathbf{j}_{\mathbf{r}}^{(\omega)}, \quad (10)$$

where $\mathbf{j}_{\mathbf{r}}^{(0)}$ is the current in the absence of microwave irradiation and thermal excitation, $\mathbf{j}_{\mathbf{r}}^{(t)}$ is the thermoinduced current, and $\mathbf{j}_{\mathbf{r}}^{(\omega)}$ is the microwave-induced current. In the linear response regime, $\mathbf{j}_{\mathbf{r}}^{(0)}$ is proportional to the gradient of electrochemical potential $\eta_{\mathbf{r}}$ according to $\mathbf{j}_{\mathbf{r}}^{(0)} = -\hat{\sigma}^{(0)} \nabla \eta_{\mathbf{r}}/e$, where $\hat{\sigma}^{(0)} = \sigma_d - \hat{\epsilon} \sigma_H$ is the conductivity tensor in magnetic field. In particular, $\sigma_H = e^2 n/m\omega_c$ is the Hall conductivity, $\hat{\epsilon}$ is the 2×2 Levi-Civita matrix,

$$\sigma_d = \sigma_0 \int d\varepsilon \left(-\frac{\partial f_\varepsilon}{\partial \varepsilon} \right) D_\varepsilon^2 \quad (11)$$

is the longitudinal (dissipative) conductivity, and $\sigma_0 = e^2 n / m \omega_c^2 \tau_{tr}$ is its classical part expressed through the transport time τ_{tr} . We consider the case of a classically strong magnetic field, $\omega_c \tau_{tr} \gg 1$, relevant for high-mobility electron gas. If η is constant, the current $\mathbf{j}_r^{(0)}$ is zero.

The thermoinduced current in GaAs quantum wells is dominated by phonon drag contribution. In general, this current is modified in the presence of microwave irradiation [25], but the effect is small compared to the influence of microwaves on the resistivity and will be neglected in the following. Using the model of bulk phonons with a three-dimensional wave vector $\mathbf{Q} = (\mathbf{q}, q_z)$ and taking into account that the scattering of electrons by phonons is quasi-elastic because of the smallness of the phonon energies compared to Fermi energy, one gets [25]

$$\begin{aligned} \mathbf{j}_r^{(t)} = & \frac{|e| k_F^2 m}{4\pi^3 \hbar^4 \omega_c^2} \int_0^{2\pi} d\varphi \int_0^\pi d\zeta \sin^{-2} \zeta \\ & \times \sum_\lambda \int_0^\pi \frac{d\theta}{\pi} (1 - \cos \theta) C_{\lambda \mathbf{Q}} I_{q_z} N_{\lambda \mathbf{Q}}(\mathbf{r}) \int d\varepsilon D_\varepsilon \\ & \times \sum_{l=\pm 1} l D_{\varepsilon - l\hbar\omega_{\lambda \mathbf{Q}}} (f_{\varepsilon - l\hbar\omega_{\lambda \mathbf{Q}}} - f_\varepsilon) [\tau_{tr}^{-1} D_\varepsilon \mathbf{n}_\varphi - \omega_c \hat{\mathbf{e}} \mathbf{n}_\varphi], \end{aligned} \quad (12)$$

where $k_F = \sqrt{2\pi n}$ is the Fermi wavenumber, λ is the mode index, φ is the polar angle of \mathbf{q} , ζ is the inclination angle, and θ is the scattering angle. The phonon frequency is given by $\omega_{\lambda \mathbf{Q}} = s_\lambda \sqrt{q^2 + q_z^2}$, where $q = 2k_F \sin(\theta/2)$ and $q_z = q \cot \zeta$. The function $C_{\lambda \mathbf{Q}}$ is the squared matrix element of the electron-phonon interaction in the bulk, comprising deformation-potential and piezoelectric-potential mechanisms (the detailed expression can be found, for example, in Ref. 25). The squared overlap integral I_{q_z} is defined as $I_{q_z} = |\int dz e^{iq_z z} F^2(z)|^2$, where $F(z)$ is the ground-state wavefunction describing confinement of electrons in the quantum well. Next, $\mathbf{n}_\varphi = (\cos \varphi, \sin \varphi)$ is a unit vector along \mathbf{q} . The current $\mathbf{j}_r^{(t)}$ is determined by the distribution function of phonons, $N_{\lambda \mathbf{Q}}(\mathbf{r})$, which depends on the heater temperature T_h and on all the details of the sample geometry and composition. In spite of the fact that this function is unknown, Eq. (12) can be rewritten in the general linear form

$$\mathbf{j}_r^{(t)} = \hat{\mathcal{B}} \mathbf{G}_r, \quad \mathbf{G}_r = -\nabla \mathcal{T}_r, \quad (13)$$

where \mathbf{G} is a potential field proportional to the frictional drag force inflicted by the in-plane component of phonon flux and \mathcal{T} is a scalar potential associated with this field. The symmetry properties of the tensor $\hat{\mathcal{B}}$ are the same as those of the conductivity tensor: $\hat{\mathcal{B}} = \mathcal{B}_d - \hat{\epsilon} \mathcal{B}_H$, \mathcal{B}_d is even in B , \mathcal{B}_H is odd in B , and $|\mathcal{B}_H| \gg |\mathcal{B}_d|$ under the assumed condition of a classically strong magnetic field. Under certain approximations, when $N_{\lambda \mathbf{Q}}(\mathbf{r}) \propto \mathbf{q} \cdot \nabla T$, one may identify \mathcal{T} with temperature T . In this case, $\hat{\mathcal{B}}$ is the thermoelectric tensor $\hat{\beta}$; see Ref. 25 for the theory of phonon-drag thermoelectric effect in a quantizing

magnetic field. Both \mathcal{B}_d and \mathcal{B}_H contain classical (non-oscillating) and quantum (oscillating with B) contributions, the latter include the magnetophonon oscillations.

Finally, the microwave irradiation adds a photocurrent whose most essential part is proportional to the gradient of electrostatic potential [3], [16]. At low temperatures of 1-2 K, when the inelastic mechanism [7] of MW-induced photocurrent dominates, the whole photocurrent is proportional to $\nabla \phi$, so we write

$$\mathbf{j}_r^{(\omega)} = -\sigma_\omega \nabla \phi_r. \quad (14)$$

Since the term $\mathbf{j}_r^{(\omega)}$ leads to violation of the Einstein relation between conductivity and the diffusion coefficient, the quantity σ_ω has been named by the authors of Ref. 16 as anomalous conductivity. In the case of weak excitation, when the response is linear in MW power, the anomalous conductivity is given by the expression

$$\sigma_\omega = \sigma_0 \frac{\tau_{in}}{4\tau_{tr}} P_\omega \int d\varepsilon D_\varepsilon^2 \sum_{l=\pm 1} \frac{\partial D_{\varepsilon + l\hbar\omega}}{\partial \varepsilon} (f_{\varepsilon + l\hbar\omega} - f_\varepsilon), \quad (15)$$

where τ_{in} is the inelastic scattering time, $P_\omega = (2e^2 E_\omega^2 \mu / m \hbar^2 \omega^2) (|s_+|^2 + |s_-|^2)$ is a dimensionless function proportional to the MW power absorbed by 2D electrons, E_ω is the MW electric field, $s_\pm = (e_x \pm ie_y) / [\sqrt{2}(\omega \pm \omega_c + i\omega_p)]$, \mathbf{e} is the unit vector of MW polarization, and $\omega_p = 4\pi e^2 n / [mc(1 + \sqrt{\epsilon_0})]$ is the radiative decay rate. In the systems with uniform electron density and temperature, where the chemical potential is constant, one has $e\nabla \phi_r = \nabla \eta_r$, so the conductivity σ_ω is simply added to σ_d and the response is determined by the total MW-modified dissipative conductivity $\sigma_d + \sigma_\omega$. If the chemical potential depends on coordinate, the response depends separately on σ_d and σ_ω .

Since no current is injected into the 2D system through the contacts, one may write

$$\oint d\mathbf{l} \cdot \hat{\epsilon} \mathbf{j}_r = 0. \quad (16)$$

where the integral is taken along any closed contour in the 2D plane. Equation (16) is the integral form of the continuity equation $\nabla \cdot \mathbf{j}_r = 0$. It means that the total current flowing in or out of the area encircled by a closed contour is zero. With the use of Eq. (2), expressions for the currents, and the identity $\oint d\mathbf{l} \cdot \nabla \eta_r = 0$ providing continuity of η_r , one may rewrite Eq. (16) as

$$\begin{aligned} & \oint d\mathbf{l} \cdot \hat{\epsilon} \left[(\sigma_d + \sigma_\omega) \nabla \eta_r \right. \\ & \left. - \sigma_\omega \left(\frac{\partial \mu}{\partial n} \nabla n_r + \frac{\partial \mu}{\partial T} \nabla T_r \right) - e \mathbf{j}_r^{(t)} \right] = 0. \end{aligned} \quad (17)$$

In our experimental setup, the electron density n changes in a narrow, determined by the distance d_G , region near the edge of the gate. In the presence of microwaves, this causes a corresponding jump of the electrochemical potential. To show this, we consider two closely spaced

contours congruent with the shape of the gate near the gate edge, a contour under the gate and another contour C_1 outside the gate, and integrate Eq. (17) between these contours. Neglecting a possible change of temperature and contribution of therminduced currents in the narrow interval of integration, we obtain

$$e(V - V_1) = \frac{\sigma_\omega}{\sigma_d + \sigma_\omega} \left(\frac{\partial n}{\partial \mu} \right)^{-1} \delta n, \quad (18)$$

where V_1 is the voltage outside the gate in the near-gate region, formally obtained by averaging of the electrochemical potential over the contour C_1 (see Fig. 4). The fact that Eq. (18) does not contain the Hall conductivity is related to the Corbino-like geometry of the experiment. However, in the presence of microwaves, when $V \neq V_1$, a large non-dissipative Hall current proportional to σ_H circulates along the gate edge.

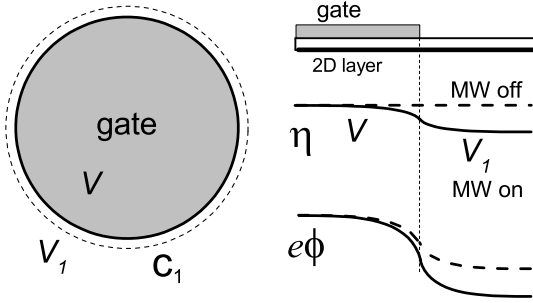


FIG. 4: Charging in the presence of microwaves. Left: schematic top view, right: spatial dependence of electrochemical and electrostatic potentials. When the gate is biased, the electron density under the gate becomes different from the density outside the gate, and the electrostatic potential is changed near the gate edge. The electrochemical potential is constant since the current must be zero. When the sample is irradiated by microwaves, the condition of zero dissipative current requires a change of electrochemical potential near the gate edge.

In the absence of non-equilibrium phonon fluxes and temperature gradients, the electrochemical potentials are equal to V and V_1 in the whole regions under the gate and outside the gate, respectively. Consequently, the variation of the voltage at the contact, δV_0 , is equal to the variation of the voltage outside the gate, δV_1 , and we obtain

$$\delta Q = C_{MW} \delta V_0 \quad (19)$$

with the MW-modified capacitance

$$C_{MW} = C_0 \left[1 + \frac{\sigma_d}{\sigma_d + \sigma_\omega} \frac{C_0}{e^2 A} \left(\frac{\partial n}{\partial \mu} \right)^{-1} \right]^{-1}. \quad (20)$$

To solve the problem in the presence of external heating, we notice that since the heater area extends over the gate region, one can expect nearly uniform heating and non-essential phonon drag in the gate region. This means that the electrochemical potential under the gate is still uniform and equal to eV . In the region out of the gate, the electrochemical potential changes because of the thermoelectric effect. This potential can be found from the continuity equation $\nabla \cdot \mathbf{j}_r = 0$ with boundary conditions expressing zero current normal to the sample boundary at this boundary and the equality $\eta_r = eV_1$ near the gate edge, $\mathbf{r} \in C_1$. As the current is given by the expression

$$\mathbf{j}_r = -\frac{1}{e} [\sigma_d + \sigma_\omega - \sigma_H \hat{\epsilon}] \nabla \eta_r + \sigma_\omega \frac{1}{e} \frac{\partial \mu}{\partial T} \nabla T_r - (\mathcal{B}_d - \mathcal{B}_H \hat{\epsilon}) \nabla T_r, \quad (21)$$

the continuity equation becomes the Poisson-like equation $(\sigma_d + \sigma_\omega) \nabla^2 \eta_r = \sigma_\omega (\partial \mu / \partial T) \nabla^2 T_r - e \mathcal{B}_d \nabla^2 T_r \equiv \nabla^2 \Phi_r$. This equation has an obvious solution (here Φ_1 is Φ_r at $\mathbf{r} \in C_1$):

$$\eta_r = eV_1 + \frac{\Phi_r - \Phi_1}{\sigma_d + \sigma_\omega} \quad (22)$$

which satisfies the boundary conditions in a particular case when both the sample and the heater are radially symmetric (Corbino geometry [28 - 30]) and describes the distribution with zero azimuthal gradients of η_r and zero radial current in any point of the sample. Despite a different geometry of our sample (Fig. 5), the solution (22) still remains valid at the symmetry axis Ox because the symmetry requires $[\nabla_y \eta_r]_{y=0} = 0$. Therefore, by using Eq. (22) one can calculate the voltage difference $V_2 - V_1$, where V_2 is the voltage at the boundary point $\mathbf{r} = (L/2, 0)$ (see Fig. 5). To find the bias $V_0 - V_2$, we write the boundary condition for the x component of the current at $x = L/2$: $j_r^x|_{x=L/2} = 0$. In the case of classically strong magnetic fields, the main contribution to the current comes from its Hall component, and the boundary condition is approximately rewritten as $[\sigma_H \nabla_y \eta_r + e \mathcal{B}_H \nabla_y T_r]_{x=L/2} \simeq 0$. This leads to the relation $V_0 - V_2 = -(\mathcal{B}_H / \sigma_H) (\mathcal{T}_0 - \mathcal{T}_2)$, where \mathcal{T}_0 and \mathcal{T}_2 correspond to the boundary points $(L/2, L/2)$ and $(L/2, 0)$ with the voltages V_0 and V_2 , respectively.

In summary,

$$V_{10} \equiv V_1 - V_0 \simeq -\frac{\mathcal{B}_H (\mathcal{T}_2 - \mathcal{T}_0)}{\sigma_H} - \frac{\mathcal{B}_d (\mathcal{T}_1 - \mathcal{T}_2)}{\sigma_d + \sigma_\omega} + \frac{1}{e} \frac{\sigma_\omega}{\sigma_d + \sigma_\omega} \frac{\partial \mu}{\partial T} (\mathcal{T}_1 - \mathcal{T}_2). \quad (23)$$

Although this expression contains a number of unknown parameters, it gives a complete account for the dependence of therminduced voltage on the MW-induced conductance contribution σ_ω . Finally, a unified expression

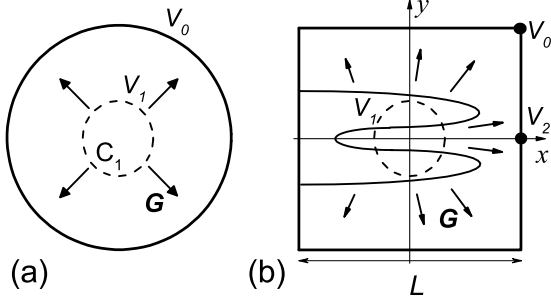


FIG. 5: Thermoelectric effect in the simple Corbino geometry (a) and in the actual geometry of the sample (b). The arrows show the distribution of phonon drag forces and temperature gradients. The meander in (b) schematically represents the heater.

relating the charging δQ with the external perturbations is written in the following way

$$\delta Q = C_{MW} \left[\delta V_0 + \delta V_{10}(T_h) - \frac{1}{e} \frac{\partial \mu}{\partial T} \delta T(T_h) \right], \quad (24)$$

where we have emphasized that the variations of the temperature of electron gas under the gate, δT , and variations of thermoelectric voltage, δV_{10} , are functions of the heater temperature T_h .

In conclusion, the capacitive response of 2D electrons is determined not only by the thermodynamic quantities $\partial n / \partial \mu$ and $\partial \mu / \partial T$ but also by the transport properties. The recharging current Eq. (1) appearing as a response to weak periodic modulation of the voltage, $V_0(t) = \Delta V \cos(\omega_0 t)$, is linear in the perturbation ΔV and determined by the capacitance C_{MW} which depends on thermodynamic density of states $\partial n / \partial \mu$ and anomalous conductivity σ_ω . The recharging current caused by a periodic perturbation of heater temperature, $T_h(t) = T_{h0} + \Delta T_h \cos(\omega_0 t)$, depends on the capacitance C_{MW} , entropy density $-\partial \mu / \partial T$, and the thermoelectric voltage δV_{10} . In the case of $\Delta T_h \ll T_h - T$, this current is linear in the perturbation ΔT_h .

Under conditions $X_k = 2\pi^2 kT / \hbar \omega_c \gg 1$, the thermal smearing of the Fermi distribution leads to $\partial n / \partial \mu = \rho_{2D}$ and $\partial \mu / \partial T = 0$. The electron density of states cannot be probed by the capacitive response in this regime. Nevertheless, the MW-induced features in the recharging current persist, and Eq. (24) is rewritten in a simpler form

$$\delta Q = C_0 \frac{\delta V_0 + \delta V_{10}(T_h)}{1 + (a_B / 4d_G) / (1 + \sigma_\omega / \sigma_d)}, \quad (25)$$

where $a_B = \hbar^2 \epsilon_0 / m e^2$ is the Bohr radius. The quantity δV_{10} is also simplified in these conditions. Moreover, if we

neglect the contribution of magnetophonon oscillations [31], which is justified in the case of low temperatures [25] and is applicable to our experiment since the amplitude of the oscillations is much smaller than the background, δV_{10} is written as

$$\delta V_{10}(T_h) \simeq \frac{v_{12}(T_h)}{1 + \sigma_\omega / \sigma_d} + v_{20}(T_h), \quad (26)$$

where v_{12} and v_{20} are B -independent voltages describing classical phonon drag contributions. In particular, under condition that $N_{\lambda \mathbf{Q}}(\mathbf{r}) \propto \mathbf{q} \cdot \nabla T$, one has $v_{12} = -\alpha(T_1 - T_2)$ and $v_{20} = -\alpha(T_2 - T_0)$, where T_1 is the temperature under the gate, T_2 and T_0 are the temperatures in the points $(L/2, 0)$ and $(L/2, L/2)$, respectively (see Fig. 5), and α is the classical phonon-drag thermopower.

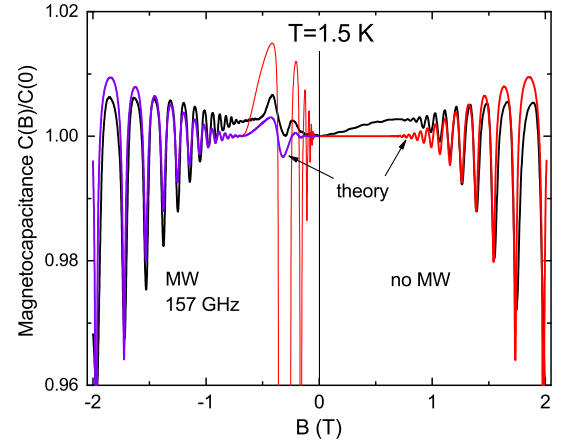


FIG. 6: (Color online) Comparison of calculated and experimental magnetocapacitance. The right and the left parts show the dark and MW-modified capacitance, respectively. In the left, two calculated plots are presented, the one given by the thicker line corresponds to inhomogeneous suppression of anomalous conductivity: σ_ω is divided by the factor ξ defined by Eq. (27).

In spite of the smallness of the geometrical factor $a_B / 4d_G \simeq 0.02$, the MW-modified capacitance C_{MW} is expected to change strongly compared to C_0 when the total dissipative conductivity $\sigma_{tot} = \sigma_d + \sigma_\omega$ becomes small compared to σ_d . Furthermore, for zero conductance ($\sigma_{tot} = 0$) corresponding to the zero resistance state realized in our samples, C_{MW} formally goes to zero. However, we need to emphasize that the theory given above cannot be applied in the intervals of magnetic fields where the resistance is zero, because the distribution of currents and fields in these conditions is far from the quasi-equilibrium one and is likely shaped into domain structures [32].

The result of the calculation of the capacitance according to Eq. (20) is shown in Fig. 6. The density of states needed for calculation of $\partial n / \partial \mu$, σ_ω , and σ_d was described in the self-consistent Born approximation based

on the quantum lifetime of electrons of 7 ps, which is a typical value for our samples at low temperatures. The amplitude of fluctuations of chemical potential, $\Gamma = 0.9$ meV, was found from fitting the amplitudes of calculated and measured oscillations of the dark capacitance. Weak oscillations of the chemical potential with magnetic field have been also taken into account. The inelastic scattering time was estimated according to $\hbar/\tau_{in} \simeq T^2/\mu$ [7]. The amplitude of the microwave field, E_ω , was chosen in such a way to obtain the closest correspondence between the measured and calculated magnetoresistance. The theory describes the general behavior of the capacitance and periodicity of the MW-induced oscillations. However, the amplitudes of the calculated MW-induced oscillations are much larger than the observed ones. These deviations are expectable from the theoretical point of view since the photovoltage associated with the anomalous conductivity σ_ω develops on short length scales, near the gate edge. Below we discuss this point in more detail.

We believe that the main reason for the small amplitudes of the observed oscillations is a suppression of the influence of microwaves on 2D electron distribution in the presence of spatial inhomogeneity near the gate edge. Indeed, while in the homogeneous case, the energy relaxation of photoexcited electrons is determined by inelastic scattering only; the relaxation of a spatially inhomogeneous distribution of electrons can also occur via spatial diffusion. This effect is roughly described in terms of the enhancement of the inelastic relaxation rate according to the substitution

$$\frac{1}{\tau_{in}} \rightarrow \frac{1}{\tau_{in}} + \frac{D}{\ell^2} = \frac{\xi}{\tau_{in}}, \quad \xi = 1 + \frac{l_{in}^2}{\ell^2}, \quad (27)$$

where ℓ is a characteristic scale of the inhomogeneity, $D = v_F^2/2\omega_c^2\tau_{tr}$ is the diffusion coefficient (v_F is the Fermi velocity), and $l_{in} = \sqrt{D\tau_{in}}$ is the inelastic diffusion length [33]. Since the anomalous conductivity σ_ω is proportional to τ_{in} , it will be suppressed as a whole by the factor ξ . In the MIRO region of magnetic fields, $B \sim 0.2 - 0.5$ T, l_{in} is of the order of $1 \mu\text{m}$. By choosing $\ell = 0.22 \mu\text{m}$, we obtain a reasonably good agreement between theory and experiment (see Fig. 6). The spatial inhomogeneities of the potentials near the gate edge can appear because of gate fabrication imperfections. Apart from this, screening of the MW field by the metallic gate can lead to a strong spatial inhomogeneity of the MW intensity near the gate edge, which in turn contributes to inhomogeneity of the electron distribution. Finally, one cannot exclude inhomogeneities caused by nonlinear effects together with a dependence of the conductivities σ_ω and σ_d on the applied voltage variations δV_0 , though we did not see direct indications of nonlinear behavior in our experiment. The suppression described by Eq. (27) also explains why there is no indication of zero resistance states in the capacitance signal.

We expect it is technically possible to reduce the suppression of the MW-induced capacitance oscillations by increasing the distance to the gate, because an increase

in d_G leads to increasing length ℓ and, consequently, to a reduction of the factor ξ . The positive effect of this modification, however, would be partly compensated by the overall decrease of the magnetocapacitance signal because of the decrease in the geometric capacitance C_0 .

A strong suppression of MIRO in spatially-inhomogeneous 2D electron gas was observed previously in the samples patterned by antidot lattice with a period of the order of $1 \mu\text{m}$ [34]. This effect could not be attributed to lowering mobility in the patterned samples, as the change in mobility compared to unpatterned samples was small. The suppression of MIRO in Ref. 34 actually can be explained by the spatial diffusion mechanism described above. Thus, the observation of the authors of Ref. 34 adds more confidence to the above interpretation of our experimental results.

Now we proceed to discussion of the response to thermal modulation presented in Fig. 3. In contrast to the case of voltage modulation, the effect of microwaves on the charging current is strong and apparently not related to weak oscillations of the capacitance discussed above. The theory suggests that the result of our observation can be understood as the influence of microwaves on the magnetothermoelectric effect in Corbino geometry, when the thermopower or, more generally, the thermoinduced voltage, is inversely proportional to dissipative conductivity [28-30]. According to Eqs. (23) and (26), the MW-induced oscillations of the conductivity contained in σ_ω are seen in the thermoinduced voltage as inverted oscillations, where maxima are replaced by minima and vice versa. Indeed, by applying the simple result of Eq. (26) with the ratio v_{12}/v_{20} as a fitting parameter to the interpretation of our experimental data, a reasonable agreement between the theory and the experiment can be reached. The exception is the region of zero conductance, where the theory is not applicable. The finite value of the charging voltage peak corresponding to a zero resistance state can be explained by nonlinear effects which become increasingly important when σ_{tot} goes to zero or, even more likely, by transport anisotropy. The latter means that the symmetry properties of thermoelectric tensor are modified, and this can have a dramatic effect on thermoelectric phenomena under condition of classically strong magnetic fields [35]. Indeed, we see a presence of antisymmetric in B contributions in the charging voltage signal, which can be a consequence of the anisotropy. We leave this problem for further study. The influence of anisotropy on thermopower in Corbino geometry has been already detected experimentally [28] but was not studied systematically. We note that application of MW irradiation allows us to study the region of relatively weak magnetic fields, whereas the previous measurements of thermopower in Corbino geometry [28,30] demonstrated peculiarities of thermoelectric response only in the quantum Hall regime.

IV. SUMMARY AND CONCLUSIONS

In this work, we explored the influence of microwaves on high-mobility 2D electron gas in a GaAs quantum well layer partly covered by the gate. The capacitive coupling of electrons to the gate placed in the center of the square sample allowed us to measure the recharging current as a result of low-frequency modulation of the voltage between the gate and one of the contacts. In this way, the effective MW-modified capacitance has been measured directly. We also measured the recharging current as a response to periodic variations of external heating by using the electrically driven heater placed under the central part of the sample. Simultaneously, using Ohmic contacts, we measured the magnetic-field dependence of the resistance that demonstrated the microwave-induced resistance oscillations (MIRO) and zero resistance states.

We have found that in the presence of microwaves the capacitance oscillates with the magnetic field. The period and the phase of these oscillations are the same as those of MIRO, but the amplitude is much smaller. The phenomenon of microwave induced capacitance oscillations has been explained as a result of violation of the Einstein relation between conductivity and the diffusion coefficient under MW irradiation. This leads to a difference in the electrochemical potentials of 2D electrons under the gate and out of the gate so that the relation between the induced charge and the applied voltage [Eqs. (19) and (20)] is modified and becomes sensitive to MW frequency. We note that a similar physical mechanism has been proposed [16] to describe MW photovoltage oscillations [14,15] appearing under condition of a built-in electric field near the contacts (for capacitive contacts, the photovoltage was measured as a response to low-frequency modulation of microwave power). A comparison of the measured and calculated MW-modified capacitance shows that the oscillations of the measured capacitance have considerably smaller amplitudes. The discrepancy is lifted if one takes into account a suppression of the influence of microwaves on electron distribution due to spatial inhomogeneity of this distribution expected in the region near the gate edge. Thus, we believe that our findings not only demonstrate the phenomenon of MW-induced capacitance oscillations but also indicate the importance of spatial diffusion in the relaxation of energy distribution of MW-excited electrons.

We have presented a linear response theory describing the recharging current and applicable under the conditions of our experiment. In particular, the theory

includes the effects of inhomogeneous temperature and thermoinduced currents, which are missing in the previous theoretical consideration [16,33,36] of the influence of MW irradiation on spatially-inhomogeneous 2D systems. The theory suggests that the response to a thermal perturbation depends on the MW-modified capacitance described by Eq. (20). However, when the temperature gradient and non-equilibrium phonon flux are present, the response has mostly thermoelectric origin. Therefore, the main effect of the microwaves on the thermoinduced recharging current comes from the influence of microwaves on the thermoelectric effect; the latter is likely dominated by phonon drag. Whereas in our previous publication [17] we showed that MW irradiation leads to antisymmetric in B oscillating contribution of thermoelectric voltage, in the present experiment we observe a symmetric in B oscillating response in antiphase with MIRO. This difference is actually related to the difference in the experimental setups. In Ref. 17 we used Van der Pauw geometry with the heater placed outside the 2D layer, while in this study we use Corbino-like geometry, where the gate at the sample center plays the role of a capacitive contact, and the heating occurs from underneath the central part of the sample. The absence of detailed knowledge about temperature and phonon flux distribution in our samples does not allow a direct quantitative comparison of theory and experiment at this point. Nevertheless, the periodicity and the shape of the oscillations of the thermoinduced voltage clearly suggest that the signal reflects the inverse proportionality of this voltage to the dissipative conductivity modified by microwaves. In the regions of zero resistance states, the measured thermoinduced voltage shows high but finite peaks. Since the linear theory developed for macroscopically homogeneous and isotropic 2D systems is not valid in these regions, a special consideration is required to describe the height of the peaks.

Finally, we believe that our research shows that application of both capacitive and thermoelectric methods in combination with MW irradiation may considerably extend the possibilities for studies of 2D electron systems in high Landau levels. Further research, both experimental and theoretical, is required to establish the role of random inhomogeneities and anisotropy in transport and relaxation of non-equilibrium 2D electrons.

The financial support of this work by FAPESP, CNPq (Brazilian agencies) is acknowledged. O.E.R. thanks I. A. Dmitriev for a helpful discussion.

¹ M. A. Zudov, R. R. Du, J. A. Simmons, and J. L. Reno, Phys. Rev. B **64**, 201311(R) (2001); P. D. Ye, L. W. Engel, D. C. Tsui, J. A. Simmons, J. R. Wendt, G. A. Vawter, and J. L. Reno, Appl. Phys. Lett. **79**, 2193 (2001).

² R. G. Mani, J. H. Smet, K. von Klitzing, V. Narayana-murti, W. B. Johnson, and V. Umansky, Nature **420**, 646

(2002); M. A. Zudov, R. R. Du, L. N. Pfeiffer, and K. W. West, Phys. Rev. Lett. **90**, 046807 (2003).

³ I. A. Dmitriev, A. D. Mirlin, D. G. Polyakov, and M. A. Zudov, Rev. Mod. Phys. B **84**, 1709 (2012).

⁴ V. I. Ryzhii, R. A. Suris, and B. S. Shchamkhalova, Sov. Phys. Semicond. **20**, 1299 (1986).

- ⁵ A. C. Durst, S. Sachdev, N. Read, and S. M. Girvin, Phys. Rev. Lett. **91**, 086803 (2003).
- ⁶ M. G. Vavilov and I. L. Aleiner, Phys. Rev. B **69**, 035303 (2004).
- ⁷ I. A. Dmitriev, M. G. Vavilov, I. L. Aleiner, A. D. Mirlin, and D. G. Polyakov, Phys. Rev. B **71**, 115316 (2005).
- ⁸ I. A. Dmitriev, A. D. Mirlin, and D. G. Polyakov, Phys. Rev. B **75**, 245320 (2007).
- ⁹ I. A. Dmitriev, M. Khodas, A. D. Mirlin, D. G. Polyakov, and M. G. Vavilov, Phys. Rev. B **80**, 165327 (2009).
- ¹⁰ I. A. Dmitriev, A. D. Mirlin, and D. G. Polyakov, Phys. Rev. B **70**, 165305 (2004).
- ¹¹ A. D. Chepelianskii and D. L. Shepelyansky, Phys. Rev. B **80**, 241308(R) (2009).
- ¹² S. A. Mikhailov, Phys. Rev. B **83**, 155303 (2011).
- ¹³ Y. M. Beltukov and M. I. Dyakonov, Phys. Rev. Lett. **116**, 176801 (2016).
- ¹⁴ A. A. Bykov, JETP Lett. **87**, 233 (2008).
- ¹⁵ S. I. Dorozhkin, I. V. Pechenezhskiy, L. N. Pfeiffer, K. W. West, V. Umansky, K. von Klitzing, and J. H. Smet, Phys. Rev. Lett. **102**, 036602 (2009).
- ¹⁶ I. A. Dmitriev, S. I. Dorozhkin, and A. D. Mirlin, Phys. Rev. B **80**, 125418 (2009).
- ¹⁷ A. D. Levin, Z. S. Momtaz, G. M. Gusev, O. E. Raichev, and A. K. Bakarov, Phys. Rev. Lett. **115**, 206801 (2015).
- ¹⁸ T. P. Smith, W. I. Wang, and P. J. Stiles, Phys. Rev. B **34**, 2995 (1986).
- ¹⁹ V. Mosser, D. Weiss, K. v. Klitzing, K. Ploog, and G. Weimann, Solid State Commun. **58**, 5 (1986).
- ²⁰ S. V. Kravchenko, D. A. Rinberg, S. G. Semenchinsky, and V. M. Pudalov, Phys. Rev. B **42**, 3741 (1990).
- ²¹ J. P. Eisenstein, L. N. Pfeiffer, and K. W. West, Phys. Rev. Lett. **68**, 674 (1992).
- ²² G. Allison, E. A. Galaktionov, A. K. Savchenko, S. S. Sa-fonov, M. M. Fogler, M. Y. Simmons, and D. A. Ritchie, Phys. Rev. Lett. **96**, 216407 (2006).
- ²³ V. S. Khrapai, A. A. Shashkin, M. G. Trokina, V. T. Dolgoplov, V. Pellegrini, F. Beltram, G. Biasiol, and L. Sorba, Phys. Rev. Lett. **99**, 086802 (2007); Phys. Rev. Lett. **100**, 196805 (2008).
- ²⁴ A. Y. Kuntsevich, Y. V. Tupikov, V. M. Pudalov, and I. S. Burmistrov, Nature Communications **6**, 7298 (2015).
- ²⁵ O. E. Raichev, Phys. Rev. B **91**, 235307 (2015).
- ²⁶ J. Zhang, S. K. Lyo, R. R. Du, J. A. Simmons, and J. L. Reno, Phys. Rev. Lett. **92**, 156802 (2004).
- ²⁷ S. D. Bystrov, A. M. Kreshchuk, Le Taun, S. V. Novikov, T. A. Polyanskaya, I. G. Savelev, and A. Ya. Shik, Fiz. Tekh. Poluprovodn. (St. Petersburg) **28**, 91 (1994) [Semiconductors **28**, 55 (1994)].
- ²⁸ H. van Zalinge, R. W. van der Heijden, and J. H. Wolter, Phys. Rev. B **67**, 165311 (2003).
- ²⁹ Y. Barlas and K. Yang, Phys. Rev. B **85**, 195107 (2012).
- ³⁰ S. Kobayakawa, A. Endo, Y. Iye, J. Phys. Soc. Jpn. **82**, 053702 (2013).
- ³¹ Averaging over the magnetophonon oscillations in Eq. (12) is equivalent to a substitution $D_{\varepsilon - \hbar\omega_{\lambda\mathbf{Q}}} \rightarrow 1$.
- ³² A. V. Andreev, I. L. Aleiner, and A. J. Millis, Phys. Rev. Lett. **91**, 056803 (2003).
- ³³ M. G. Vavilov, I. A. Dmitriev, I. L. Aleiner, A. D. Mirlin, and D. G. Polyakov, Phys. Rev. B **70**, 161306(R) (2004).
- ³⁴ Z. Q. Yuan, C. L. Yang, R. R. Du, L. N. Pfeiffer, and K. W. West, Phys. Rev. B **74**, 075313 (2006).
- ³⁵ P. N. Butcher and M. Tsousidou, Phys. Rev. Lett. **80**, 1718 (1998).
- ³⁶ J. Dietel, L. I. Glazman, F. W. J. Hekking, and F. von Oppen, Phys. Rev. B **71**, 045329 (2005).